RF Modeling of the ITER-Relevant Lower Hybrid Antenna

J. Hillairet[a,*], S. Ceccuzzi[b], J. Belo[d], L. Marfisi[a], J.F. Artaud[a], Y.S. Bae[c], G. Berger-By[a], J.M. Bernard[a], Ph. Cara[a], A. Cardinali[b], C. Castaldo[b], R. Cesario[b], J. Decker[a], L. Delpech[a], A. Ekedahl[a], J. Garcia[a], P. Garibaldi[a], M. Goniche[a], D. Guilhem[a], G.T. Hoang[a], H. Jia[e], Q.Y. Huang[e], F. Imbeaux[a], F. Kazarian[f], S.H. Kim[a], Y. Lausenaz[a], R. Maggiora[g], R. Magne[a], S. Meschino[i], D. Milanesio[g], F. Mirizzi[b], W. Namkung[j], L. Pajewski[i], L. Panaccione[b], Y. Peysson[a], A. Saille[a], G. Schettini[i], M. Schneider[a], P.K. Sharma[h,a], A.A. Tuccillo[i], O. Tudisco[b], G. Vecchi[i], R. Villari[b], K. Vulliez[a], Y. Wu[e], Q. Zeng[e]

[a] *CEA, IRFM, F-13108 Saint-Paul-lez-Durance, France.*
[b] *Associazione Euratom-ENEA sulla Fusione, CR Frascati, Roma, Italy.*
[c] *National Fusion Research Institute, Daejeon, Korea.*
[d] *Associaï¿œao Euratom-IST, Centro de Fusao Nuclear, Lisboa, Portugal.*
[e] *Institute of Plasma Physics, CAS, Hefei, Anhui, China.*
[f] *ITER Organization, Saint-Paul-lez-Durance, France.*
[g] *Politecnico di Torino, Dipartimento di Elettronica, Torino, Italy*
[h] *Institute for Plasma Research, Bhat, Gandhinagar 382 428, Gujarat, India.*
[i] *"Roma Tre" University, Rome, Italy.*
[j] *Pohang Accelerator Laboratory, Pohang Univ. of Science and Technology, Pohang, Korea.*

Abstract

In the frame of the EFDA task HCD-08-03-01, a 5 GHz Lower Hybrid system which should be able to deliver 20 MW CW on ITER and sustain the expected high heat fluxes has been reviewed. The design and overall dimensions of the key RF elements of the launcher and its subsystem has been updated from the 2001 design in collaboration with ITER Organization. Modeling of the LH wave propagation and absorption into the plasma shows that the optimal parallel index must be chosen between 1.9 and 2.0 for the ITER Steady-State scenario. The present study has been made with $n_{\parallel} = 2.0$ but can be adapted for $n_{\parallel} = 1.9$. Individual components have been studied separately giving confidence on the global RF design of the whole antenna.

Keywords: Lower Hybrid, Current Drive, LHCD, PAM, ITER

1. Introduction

Following the ITER STAC recommendation, an EFDA task has been created in order to initiate the conceptual design, the R&D program, the procurement and the installation of a Lower Hybrid Current Drive (LHCD) system on ITER. The EFDA task HCD-08-03-01 has reported a revised 5 GHz LHCD system able to deliver 20 MW/CW on ITER and to sustain the expected high heat fluxes coming from the plasma radiation, particles fluxes and RF losses[1]. This work has been achieved in collaboration with ITER organization under worldwide contributions from China, India, Korea and USA in addition to EFDA.

In this paper, we report the work made in this Task Force concerning the design of the key RF elements of the antenna such as the Passive-Active Multijunction (PAM), the $TE_{10} - TE_{30}$ mode converter, the 3 dB splitter and the RF window. Detailed studies of the transmission lines elements can be found in [2, 3, 4]. Overall dimensions have been updated from the initial conceptual 2001 Detailed Design Description (DDD)[5]. ITER mechanical constraints, such as the port plug size or the rear flange dimensions, have been taken into account since the initial RF design. In parallel to the RF design, the coupling to the plasma of the launcher has been studied with the ALOHA, GRILL3D and TOPLHA codes and results are in good agreement[6].

*Corresponding author
Email address: julien.hillairet@cea.fr (J. Hillairet)

2. RF components description

2.1. Antenna general description

The LH launcher design presently foreseen for ITER is a Passive-Active Multijunction (PAM) concept, which have been successfully validated on FTU[7] and on Tore Supra[8]. In a PAM launcher, a passive waveguide – consisting in an equivalent electric short-circuit located at a quarter wavelength from the mouth – is inserted between two active waveguides which launch the RF power to the plasma. Cooling pipes are vertically drilled behind the passive waveguides in order to actively cool the launcher front face and the waveguide walls and damp part of the neutron flux, which is a mandatory requirement for any ITER plasma facing component.

An important parameter of the launcher is the nominal refractive parallel index $n_{\parallel}$ excited by the coupling structure[1]. Integrated simulations of propagation and absorption of LH waves in ITER for several scenarios showed that an optimum $|n_{\parallel}|$, defined as a trade-off between maximizing the current drive efficiency and minimizing the power deposition in the H-mode pedestal, is found to be $|n_{\parallel}| = [1.9 - 2.0]$ with a flexibility of $[1.8 - 2.2]$[9]. A new arrangement of PAM has been studied in order to allow a larger $n_{\parallel}$ flexibility compared to the previous design[5], i.e. increasing the peak $n_{\parallel}$ range from $[1.9 - 2.1]$ to $[1.8 - 2.2]$.

In the present design, the launcher is made of 48 identical modules, each one independently fed by one klystron: twelve in the toroidal direction and four in the poloidal direction. A module consists of four active waveguides in the toroidal direction and six lines of waveguides in the poloidal direction (Figure1). Thus, the whole launcher contains 1152 active waveguides whose dimensions are 9.25×58 mm. The RF power is carried through a transmission line up to a RF window located inside the frame and connected to a poloidal 3 dB splitter which feeds two $TE_{10} - TE_{30}$ mode converters. Each of these mode converters converts the incident power from the rectangular TE_{10} mode to the rectangular TE_{30} mode in order to divides the power into three poloidal rows, corresponding to the input of a 4-active waveguides multijunction. In this paper, we focus on the main RF components of the antenna which are under the machine vacuum: the RF window in Sec.2.2, the hybrid junction in Sec.2.3, the mode converter in Sec.2.4 and the PAM multijunction in Sec.2.5.

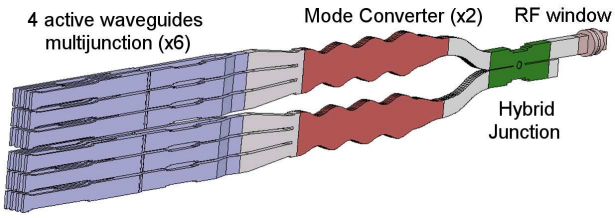

Figure 1: 3D view of one module (RF modeling): the power is coming from the right of the figure, through the RF window, the hybrid junction, the two mode converters and the six PAM multijunctions. All the elements of a module located behind the RF window are under the machine vacuum.

2.2. RF Windows

5 GHz RF windows capable of sustaining 500 kW CW are one of the most challenging RF devices of this antenna, since the ceramic used to separate the tokamak vacuum from the pressurized transmission line is a safety component and the window must handle and evacuate heat coming from dielectric and conduction RF losses. Different designs have been proposed based on pill-box geometry and cooled by a water skirt around the ceramic. A promising design, based on a WR229 cross-section input and output (58.17×29.08 mm) ensures a theoretical return loss of -34 dB and a volume integrated losses of 540 W on matched load. The ceramic is a 42.8 mm radius, 8.3 mm thick beryllium oxide disk (BeO, $\varepsilon_r = 6.7$, $\tan\delta = 4 \times 10^{-4}$). The length of the circular part of this model is 48.3 mm. The peak electric field in the vacuum part is 768 kV/m while it is 430 kV/m inside the ceramic. A thermomechanical analysis of this design can be found in reference [10]. For comparison, the simulated integrated losses into the Tore Supra 3.7 GHz windows is 760 W while the peak electric field inside is 2.1 MV/m for an input power of 250 kW.

2.3. 3 dB splitter

The aim of the 3 dB splitter is to equally split the power from a 500 kW klystron into two waveguides disposed in poloidal direction. This device is a 90° short-slot hybrid coupler[11]. The modeled WR229 device has a predicted return loss of -53 dB with an isolation of -57 dB. Its coupling factor of -3.01 ± 0.02 dB indicates that the power is well divided into the two outputs. The phase

[1] The actual $n_{\parallel}$ spectrum may vary slightly from the nominal value, depending upon plasma conditions in front of the antenna.

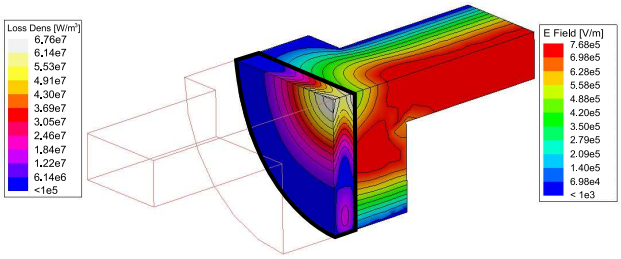

Figure 2: 3D view of the BeO window (1/4): The left colorbar represents the dielectric losses $[W/m^3]$ inside the BeO ceramic for an input power of 500 kW. The ceramic has been underlined by a black line for clarity. The right colorbar represents the associated electric field in [V/m] in the vacuum section. 5 GHz ANSOFT HFSS simulation on matched ports.

shift between the two outputs is 90°. The maximum electric field on matched ports as seen in Figure 3, is 935 kV/m for an input power of 500 kW. This value is higher than in the input straight section (752kV/m) and other design option will be studied in order to decrease this large value. For comparison, the simulated peak electric field inside the Tore Supra 3.7 GHz 3 dB hybrid junction is 725 kV/m and 566 kV/m in a straight waveguide in vacuum for a frequently reached input power of 400 kW.

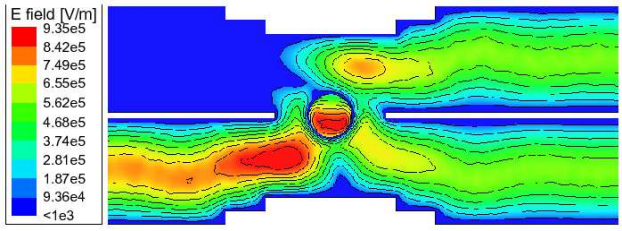

Figure 3: Side view (poloidal view) of the 3 dB hybrid junction: electric field generated inside the structure when excited by a 500 kW source. Excitation comes from the left lower part. 5 GHz ANSOFT HFSS simulation on matched ports.

2.4. $TE_{10} - TE_{30}$ mode converter

The aim of this mode converter section is to equally split the input RF power in three in the poloidal direction using a mode conversion. Such splitting scheme is achieved by perturbation of the waveguide geometry leading to mode coupling. The fundamental TE_{10} input mode can thus be almost totally converted to the TE_{30} mode, which ideally distributes the power into three rows in the H-plane. Keeping the waveguide height to 29.08 mm, the input width a_0 must be set sufficiently large in order to permit the TE_{30} mode to propagate (i.e. $a_0 \geqslant 90$ mm). In order to make the transition between this width and the input WR229 waveguide width, which is 58.17 mm, an extra taper must be added. Because of the symmetry of the device, the TE_{40} mode is not excited by the input TE_{10} and the output width a_1 is set to insure the TE_{50} mode to cut-off (i.e. $a_1 \leqslant 150$ mm). The mode evolution along the mode converter is obtained by solving the generalized telegraphist's equations for a 3.5 periods deformed waveguide of wavelength λ_w defined by the following cosinusoidal perturbation[12](Figure 4):

$$a(z) = a_0 + \varepsilon \left[1 - \cos\left(\frac{2\pi}{\lambda_w} z\right)\right] \quad (1)$$

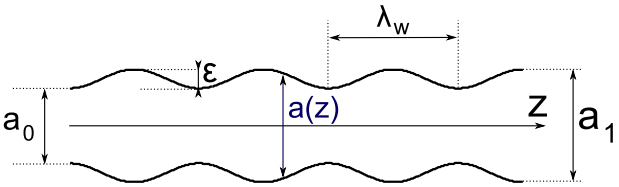

Figure 4: Schematic drawing of the $TE_{10} - TE_{30}$ mode converter.

In order to reach the highest mode conversion efficiency to the TE_{30} mode, a numerical optimization of parameters a_0, ε and λ_w has been made with Matlab. Further optimization of these parameters has been made with ANSOFT HFSS, taking into account conduction RF losses on walls and led to the following dimensions: $a_0 = 98$ mm, $\varepsilon = 22.37$ mm, $\lambda_w = 173.1$ mm and $a_1 = 142.8$ mm. The theoretical mode conversion efficiency is close to 98.65% with a return loss of -20.5 dB. Propagation losses for copper walls are 0.45%. The bandwidth of the device, defined as the range of frequencies for which at least 95% of the TE_{10} mode is converted to TE_{30}, is 115 MHz. The maximum electric field on matched ports into the mode converter is 700 kV/m as illustrated in Figure5. The total length of the mode converter with input taper is 765.7 mm. For comparison, the simulated peak electric field inside the Tore Supra 3.7 GHz mode converter is 515 kV/m for a frequently reached input power of 200 kW. A low power mock-up of this 5 GHz mode converter has been manufactured at CEA/IRFM.

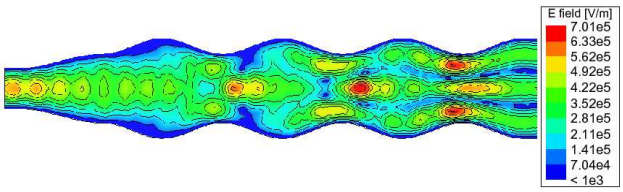

Figure 5: Side view (poloidal view) of the mode converter: electric field generated when excited by a 250 kW source. 5 GHz ANSOFT HFSS simulation on matched ports.

2.5. Passive-Active Multijunction

An illustration of the present multijunction design, with four active waveguides per toroidal line is shown in Figure 6. The passive waveguides, not illustrated in the Figure, are inserted between each active waveguides. In this design, the active waveguides ($b_a = 9.25\,\mathrm{mm}$) are wider then passive waveguides ($b_p = 7.25\,\mathrm{mm}$). The waveguides height ($a = 58\,\mathrm{mm}$) avoids the higher mode TE_{20} to propagate and is close to the WR229 standard ($58.17 \times 29.08\,\mathrm{mm}$). The structure has been optimized in order to reach the following goals: i) minimize the reflected power, ii) insure a 270° phase shift between adjacent active waveguides. The estimated return loss of the optimized structure is $-34\,\mathrm{dB}$ while the phase difference between adjacent output waveguides is 270°±0.7°. The transmitted power $|S_{n1}|^2$ (with $n = \{2, 3, 4, 5\}$) is $1/4 \pm 7 \times 10^{-3}$ which means that the input power is well divided into the 4 output of the multijunction. The maximum electric field on matched ports is 346 kV/m for a power input of 250 kW, the propagation loss $1 - \sum_n |S_{n1}|^2$ for copper walls is 1.2% and the total length of the multijunction illustrated in Figure6 is 1.170 m.

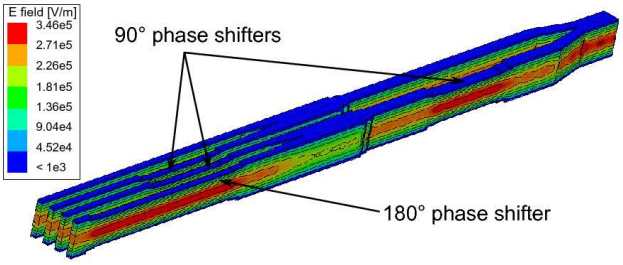

Figure 6: Electric field into the 4 active waveguides multijunction design. The input power is 83 kW, corresponding to the 250 kW incoming into the mode converter then divided by 3 in each rows of the poloidal divider. The passive waveguides located between each active waveguides are not illustrated in this picture. 5 GHz ANSOFT HFSS simulation on matched ports.

3. Conclusion

In the frame of an EFDA Topical Group, the RF design of the foreseen ITER Lower Hybrid Current Drive antenna has been updated. A new arrangement of multijunctions and power feeding has allowed an increase of the flexibility of the launched peak parallel index in comparison to the previous design. The main RF components of the launcher subsystem such as the RF windows, the hybrid junction, the mode converter and the multijunction, have been studied and optimized separately and a mode-converter mock-up has been manufactured at CEA/IRFM. The good theoretical results obtained give confidence on the global RF design of the LH launcher. Further work will concentrate on thermo-mechanical analysis of the different parts, neutron shielding and total length reduction of the antenna in order to satisfy the ITER constraints.

Acknowledgments

This work, supported by the European Communities under the contract of Association between EURATOM and CEA, was carried out within the framework of the EFDA task HCD-08-03-01. The views and opinions expressed herein do not necessarily reflect those of the European Commission

References

[1] G. Hoang, et al., A Lower Hybrid Current Drive System for ITER, Nuclear Fusion 49 (075001).

[2] F. Mirizzi, et al., Design of the Main Transmission Line for the ITER Relevant LHCD System, in: 26th SOFT, 2010.

[3] S. Ceccuzzi, et al., Mode filters for oversized transmission lines, in: 26th SOFT, 2010.

[4] S. Meschino, et al., Bends in oversized rectangular waveguide, in: 26th SOFT, 2010.

[5] P. Bibet, et al., Toward a LHCD system for ITER, Fusion Engineering and Design 74 (1-4) (2005) 419 – 423, ISSN 0920-3796, proceedings of the 23rd Symposium of Fusion Technology - SOFT 23.

[6] D. Milanesio, et al., Benchmark Of Coupling Codes (ALOHA, TOPLHA, GRILL3D) With Lower Hybrid Antenna, in: 26th SOFT, 2010.

[7] V. Pericoli-Ridolfini, et al., LHCD and coupling experiments with an ITER-like PAM launcher on the FTU tokamak, Nuclear Fusion 45 (9) (2005) 1085.

[8] A. Ekedahl, et al., First experiments with the ITER-relevant LHCD launcher in Tore Supra, in: 37th EPS Conference on Plasma Physics, Dublin, 2010.

[9] A. Becoulet, et al., Steady State Long Pulse Tokamak Operation Using Lower Hybrid Current Drive, in: 26th SOFT, 2010.

[10] L. Marfisi, et al., Mechanical modeling of ITER LHCD antenna elements, in: 26th SOFT, 2010.

[11] Y. S. Bae, et al., Design of 5.0-GHz KSTAR lower-hybrid coupler, Fusion Engineering and Design 65 (4) (2003) 569 – 576, ISSN 0920-3796.

[12] P. Bibet, T. Nguyen, J. Achard, G. Berger-By, S. Berio, M. Goniche, G. Rey, G. Tonon, Experimental and Theoretical Results Concerning the Development of the Main RF Components for Nest Tore Supra LHCD Antennae, in: Proceeding of the 18th SOFT Conference, vol. 1, 1994.